

Measurement of Transonic Dips in the Flutter Boundaries of a Supercritical Wing in a Wind Tunnel

A J Persoon,* J J Horsten,* and J J Meijer†

National Aerospace Laboratory (NLR), Amsterdam, The Netherlands

Flutter experiments were performed on a supercritical transport type wing to investigate the transonic dip in the flutter boundaries and to obtain data for verification of a calculation method for unsteady aerodynamic loads. Complete transonic dips were measured at three wing angles of attack. At the highest wing angle of attack, a second dip was found. Simultaneously, the mean pressure distribution was measured in one chordwise section which could explain the flutter characteristics. Using a flutter damper device, flutter onset could be measured accurately and rapidly. This paper deals with the experimental test setup, describes the on line data reduction, and presents the results.

Nomenclature

c/c_r	= damping ratio (percent of critical damping)
C_p	= mean pressure coefficient
$C_{p0.95}$	= mean pressure coefficient at 95% of chord
f	= model frequency
M_{11} M_{22}	= modal mass of modes 1 and 2, respectively
M_∞	= Mach number
P_0	= stagnation pressure
x/c	= dimensionless chord
α_0	= adjusted wing angle of attack
α_w	= measured wing angle of attack

I Introduction

DURING the last decade a large part of the aeroelastic investigations at the National Aerospace Laboratory (NLR) focused on the determination of unsteady airloads on oscillating supercritical wings in transonic flow.¹ These investigations aimed to contribute to the development of an advanced short to-medium haul transport aircraft to be built by the Netherlands Aircraft Factories Fokker B V. One of the topics was the development of an engineering type method at NLR for three dimensional unsteady transonic airloads applicable to large aspect ratio wings to be used in the prediction of flutter boundaries in transonic flow. In summary, this method combines calculations of aerodynamic loads on oscillating two dimensional (2 D) wings in transonic flow with three dimensional (3 D) corrections due to wing span and taper calculated with 2 D and 3 D doublet-Lattice methods. An outline of this so called quasi three dimensional (Q3D) method is given in Ref. 2.

An experimental validation of the Q3D method was considered necessary. The most direct way would have been the performance of pressure measurements on an oscillating model, but a flutter model test was preferred because transonic flutter characteristics of the wing could be studied, especially the presence of transonic dips in the flutter boundaries. For that reason it was decided to perform a flutter test on a supercritical wing model for which many data

of steady pressure model tests were available already. The flutter model was designed as a study model and did not represent the aeroelastic behavior of any full-scale design.

The first flutter test was carried out in 1979 in the high speed wind tunnel (HST) of NLR with partial success. In particular, complete transonic dips could not be measured because of unexpected instabilities at low Reynolds numbers.² After modification of the model a second flutter test was carried out in the same wind tunnel in April 1982. An improved data acquisition and reduction system also was used. This investigation was very successful. The principal demands made upon the test setup were:

1) The validation of the Q3D method would be performed mainly by correlating measured and calculated flutter boundaries, which led to the design requirement that the flutter boundaries should lie within operational limits of the wind tunnel. The transonic dip should not be measured at a Reynolds number that is too low to avoid ineffectiveness of the transition strip.²

2) All data necessary for validation of the Q3D method had to be measured (during wind off: the vibrational characteristics of the model; during wind on: frequencies and damping values of the model response, mean flow condition, onset of flow separation and wing angle of attack).

3) Establishing an accurate flutter boundary required a flutter damper as a safety device during measurements at zero decay of the model response.

4) To allow for any unforeseen aeroelastic behavior of the model, especially around the transonic dip, an on line presentation of the model flutter characteristics was required.

This paper deals mainly with the experimental test setup and the measuring equipment. In addition, a number of interesting results showing the transonic dips are presented while computations derived from the subsonic lifting surface theory (doublet lattice) have been added for comparison. The comparison with calculated flutter characteristics based on the Q3D method and other methods is the subject of a subsequent paper.³

II Test Setup

Wind Tunnel

The experiments were carried out in the transonic wind tunnel HST⁴ where the Mach number could be increased up to $M_\infty = 1.35$, while the stagnation pressure could be varied between $P_0 = 12.5$ and 400 kPa. The 2.00×1.60 m² rectangular test section is provided with slotted upper and lower walls with an open area ratio of 12.5%.

Presented as Paper 83-1031 at the AIAA/ASME/ASCE/AHS 24th Structures, Structural Dynamics and Materials Conference, Lake Tahoe, Nev., May 2-4, 1983; received Sept. 10, 1983; revision received May 30, 1984. Copyright © American Institute of Aeronautics and Astronautics, Inc. 1984. All rights reserved.

*Research Engineer, Department of Aeroelasticity.

†Senior Research Engineer, Department of Aeroelasticity.

Wing Model

The test object was a semispan model of a supercritical transport type wing with an aspect ratio of 11 and an airfoil thickness distribution of 16% at the root to 11.5% at the tip. The model was made of duraluminum and was fixed to a turntable in the wind tunnel sidewall by means of a torsional spring (Fig. 1). A half body representing the fuselage was clamped to the turntable. The X shaped torsional spring was rigid in bending and relatively flexible in torsion, so that in consequence the flutter characteristics of the model were determined by the fundamental bending of the wing and the torsion of the spring.

The spring was instrumented with strain gages. The mean values of the strain gage signals were used to measure the static deformation of the spring (α_w) and the mean aerodynamic loads in terms of lift and pitching moment coefficients. These results could be correlated with results of the earlier steady pressure model tests mentioned previously.

The dynamic part of the strain gage signals was used to determine frequency and damping values of the model. Vibration levels were detected by two accelerometers mounted at 80% semispan.

Additional information about the mean flowfield could be obtained from a wing section with 12 steady pressure orifices in the upper surface at 70% semispan. The most downstream pressure orifice was situated close to the trailing edge. In this way the onset and the progression of flow separation could be observed and correlated with changes of the flutter characteristics.

After the first flutter test, the model mass distribution was modified especially in the wing tip region to ensure that the dip in the flutter boundaries would not occur at extremely low stagnation pressures. This modification is discussed further in Sec. III.

A larger roughness of the transition strip was selected (150 grit vs 220 grit as applied during the first flutter test) as an additional precaution to ensure effectivity of the strip also at the lowest expected stagnation pressure.

Excitation of the model was provided by residual turbulence of the flow in most test runs. In a limited number of test runs linear frequency sweeps and an impulse also were used by means of two electrodynamic shakers. The purpose was to investigate different excitation techniques which required less testing time than turbulence of the flow.

To approach the flutter boundary as close as possible and in a safe way, the shakers could be switched on to act also as a flutter damper device. This method already operated perfectly during the first flutter test.

III Vibrational Characteristics of the Model

As mentioned previously, the flutter model was modified prior to the wind tunnel test. The aim was to limit the stagnation pressures at which flutter would occur. The maximum stagnation pressure was set at about 300 kPa at $M_\infty = 0.6$ to avoid overloading of the torsional spring. The minimum pressure was set at about 100 kPa in the bottom of the transonic dip to avoid time consuming evacuation of the wind tunnel duct. To meet these requirements a modification of the mass distribution in the tip region was pursued as being the most sensitive place to influence the flutter characteristics of the model.

The required modification was derived from calculations and vibration tests. In the calculations a finite element modeling of the flutter model and support was applied to determine the vibration modes. Using these results with estimated unsteady transonic airloads, the flutter boundaries were calculated. The predictions were verified extensively both in a bench test during the evaluation and in the wind tunnel. The model data were measured with a Hewlett Packard Structural Dynamics Analyzer (HP 5423 A) using an impact testing technique with an instrumented hammer. During these tests it appeared that the analyzer was not

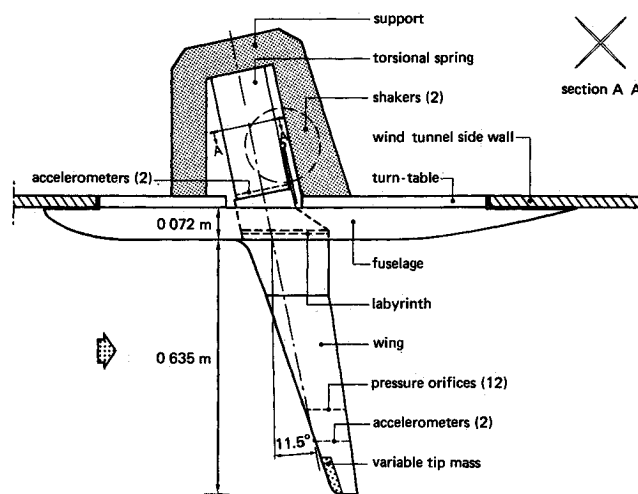


Fig 1 Global view of flutter model and support

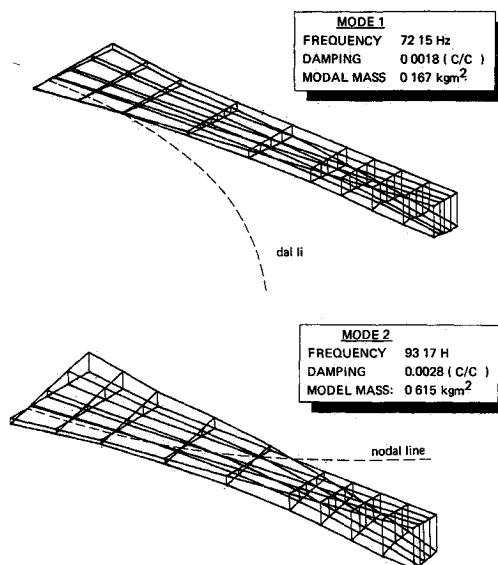


Fig 2 Vibration modes of the wing model

adequate to determine modal masses of this very lightly damped wing model. For that reason, the modal masses also were determined by measuring frequency shifts due to added small masses during sinusoidal excitation. The structural damping was verified by a decay method and agreed fairly well with the results from the impact testing technique.

From the calculations and vibration tests it appeared that adding a mass of only 5 g along the leading edge in the tip region was already sufficient. The change in model properties consisted mainly of an increase of the modal mass of mode 2, a torsion type mode. Results of the vibration tests are shown in Fig. 2.

Because of uncertainties in establishing the required modification, two other tip masses were available for a last minute adjustment in the wind tunnel.

IV Instrumentation

The basic components of the measuring equipment were the HP 5423 A Structural Dynamics Analyzer coupled to a dual disk based HP 21 MXE minicomputer (Fig. 3). The main advantage of such a setup was the possibility of acquiring wind tunnel data and model test data simultaneously on the disk of the computer under the same test identification parameters. For safety reasons, the model test data also were

stored on the magnetic tape unit of the analyzer. Appropriate software was developed to present on line flutter diagrams and mean pressure distributions. In the flutter diagrams the stagnation pressure or the Mach number could be selected as variable. In this way a rapid monitoring of frequency and damping of each vibration mode was possible. Because data reduction and on line presentation were controlled completely by the computer, more time became available to analyze the results during the tests, enabling adjustment of the test program, if necessary. It is the opinion of the authors that this data handling procedure contributed substantially to the measurement of complete transonic dips and the understanding of the flutter mechanisms during the test.

Referring again to Fig 3 the steady parts (dc) of the signals of the strain gages and scanning valve transducer were processed by the computer of the data reduction system of the HST (Quick Look) and stored on the disk of the HP 21 MXE computer. Next, the mean aerodynamic loads and the pressures were calculated and presented as well. Simultaneously, the Fourier analyzer processed a manually selected response signal. The analyzer was preprogrammed with a number of keyboard statements by which a band selectable Fourier analysis (among others) could be performed. This was required for an accurate determination of damping close to flutter onset.

If turbulence of the flow was used as a source of model excitation, the power spectrum of the model response was obtained and averaged during 60s to 80s until the shape of the spectrum became stabilized. Next, a curve fitting technique, available in the analyzer library was used to determine frequencies and critical damping ratios (see Fig 4). If it was decided to obtain similar data from a transfer function (Fig 4b) due to forced model excitation, a circle fit procedure was applied (Fig 4c). This fitting technique was also a capability of the analyzer.

After completion, the spectral data were transmitted from the analyzer to the 21 MXE computer and the values of frequencies and damping were compiled in an on line graphically displayed flutter diagram. Because the pressure distribution was also available the nature of the model response could be correlated with that of the flow directly after each test run.

Another essential part in the test setup was the flutter damper system (Fig 5). This device consisted of a feedback system on which two signals of the strain gages mounted on

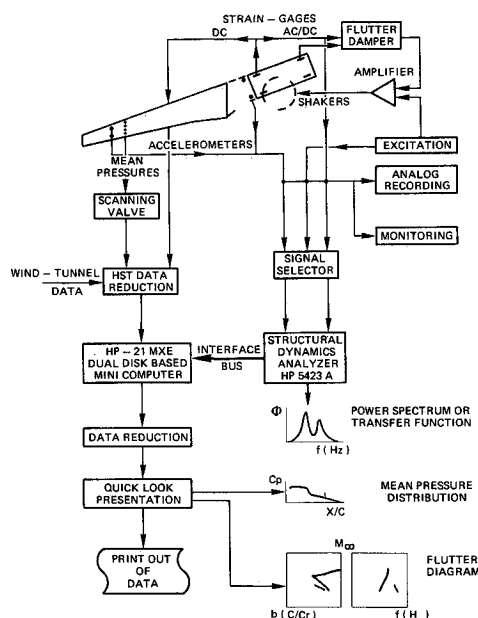


Fig 3 Scheme of measuring equipment

the spring were monitored, viz, the rotational displacement α and the maximum strain σ of the spring. If one of both signals exceeded a preset level, the damper hardware was activated, resulting in a 90 deg phase shift of the α signal. This signal was amplified and fed into both shakers so that a damping force into the model was introduced.

A demonstration of the flutter damper during the wind tunnel measurements is shown in Fig 6. Vibrations of the model just beyond flutter onset decreased rapidly by activating the damper system. With these provisions detailed flutter boundaries could be measured in a short time and in a straightforward manner.

V Test Procedure and Test Program

The test procedure (see Fig 7) to be followed depended a great deal on the shape of the flutter boundary. At subsonic Mach numbers (approximately $M_\infty = 0.6$), the stagnation pressure was the test variable. When adjusting a test con-

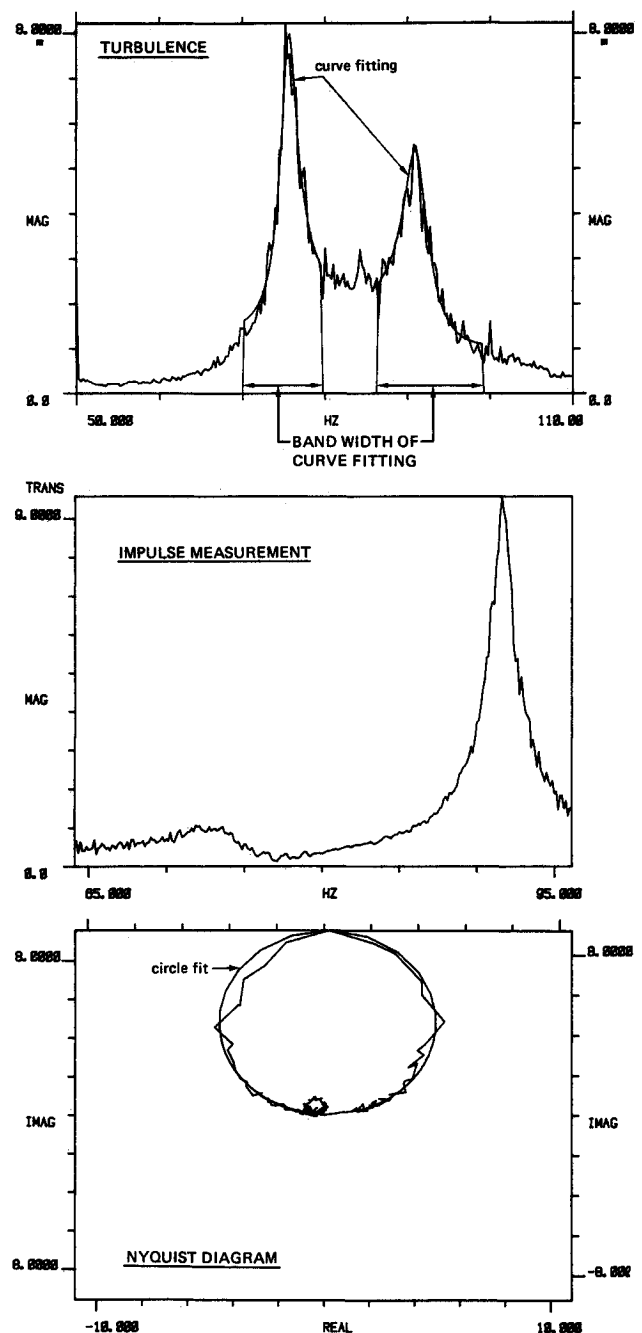


Fig 4 Curve fitting procedures

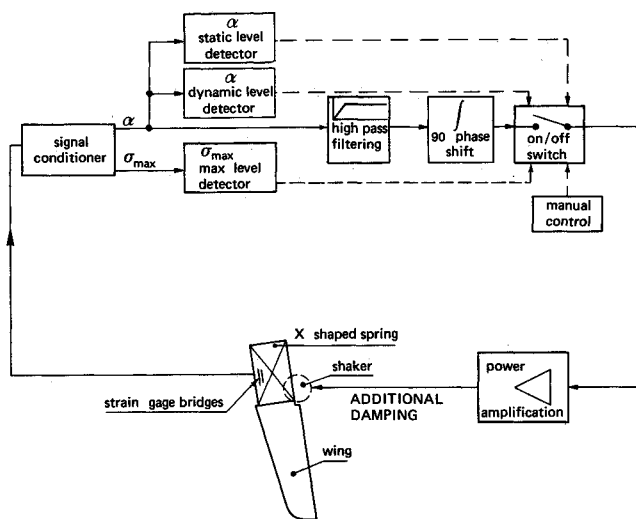


Fig 5 Flutter damper system

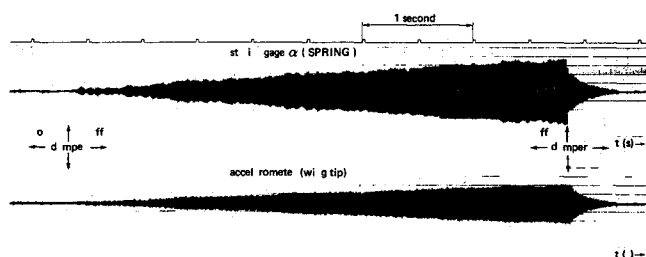
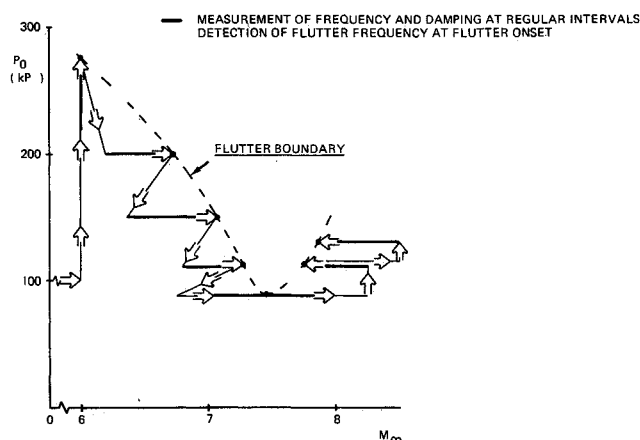
Fig 6 Demonstration of the flutter damper just beyond flutter onset ($M_\infty = 0.73$; $P_0 = 120$ kPa; $\alpha_0 = 0.85$ deg)

Fig 7 Principle of the test procedure

dition, the flutter damper was switched on. Having attained the test condition, the dampers were switched off manually. When the response of the model remained stable, frequencies and damping ratios were measured after which the damper was switched on again. After a few test points the flutter stagnation pressure was estimated with the aid of the on line flutter diagram and was thereupon verified by increasing stagnation pressure. In this way the time to settle flutter onset could be kept relatively short.

In the transonic flow regime the stagnation pressure was kept constant while the Mach number was gradually increased up to flutter onset. This method of measuring the flutter characteristics appeared to be less time consuming. Mach number sweeps were also made in the region beyond the

transonic dips, and the damper was used in the same way as described previously.

The test program covered a Mach number range of $M_\infty = 0.6$ to 0.85 at stagnation pressures of $P_0 = 80$ to 275 kPa. The adjusted wing angles of attack were $\alpha_0 = -0.35$, 0.85 , and 2.05 deg. After removing the transition strip, the condition $\alpha_0 = -0.35$ deg was measured again. During that condition frequency sweeps and an impulse also were applied as excitation techniques. The complete test program contained about 360 different test conditions measured in a four day wind tunnel test.

VI Presentation of Results

Flutter Boundaries and Frequencies

A selection of flutter diagrams, as displayed on line, is presented in Figs 8-10, showing the development of frequencies and damping ratios of both vibration modes as a function of either stagnation pressure (Fig 8) or Mach number (Figs 9 and 10).

From the results at two different wing angles of attack ($\alpha_0 = 0.85$ and 2.05 deg) in the subsonic flow regime ($M_\infty = 0.603$), a classical flutter instability can be observed (Fig 8). Increasing the stagnation pressure, mode 1 becomes unstable, while mode 2 becomes heavily damped. Figure 8 also illustrates that the flutter characteristics at both wing angles of attack are similar, as may be expected in subsonic flow.

The presence of transonic dips is clearly demonstrated in Figs 9 and 10 at wing angles of attack of $\alpha_0 = -0.35$ and 2.05 deg. In the upper diagram of Fig 9, the bottom of a dip is shown at $M_\infty \approx 0.78$ for mode 1. A slight variation in Mach number, however, leads to stable vibrations.

Similar results were obtained when the transition strip was removed (see lower diagram of Fig 9). Without transition the dip shifts to a somewhat lower Mach number. Further, rather abrupt changes in the frequencies of mode 1 occurred in contrast with the case of fixed transition.

Of much interest is Fig 10 ($\alpha_0 = 2.05$ deg), where both vibration modes become unstable at different Mach numbers. At a stagnation pressure of $P_0 \approx 140$ kPa (upper diagram), mode 1 becomes unstable first, whereas at higher Mach numbers instability of mode 2 occurs, indicating the presence of a second unstable region. Lowering the stagnation pressure to $P_0 \approx 103$ kPa (lower diagram), mode 1 remains stable throughout the Mach number range, illustrating that these measurements were performed just beneath the first transonic dip. Again, the abrupt shift in frequencies is remarkable when mode 2 tends to become unstable.

After flutter onset was measured at a large number of test conditions, the flutter boundaries were compared for the three wing angles of attack. Figure 11 shows very clearly the transonic dips and the second unstable region as measured at $\alpha_0 = 2.05$ deg. The actual wing angles of attack (α_w) are presented as well, since knowledge of these values is essential for the calculation of unsteady airloads. It should be mentioned that the bottom of the transonic dips was detected very precisely. Low damped oscillations as measured by NASA Langley⁵ were not detected.

Figure 12 shows a survey of measured flutter boundaries together with the flutter frequencies and the mean pressure coefficient at 95% chord. As can be observed, in the bottom of the dip the flutter frequencies have decreased to a value close to the natural frequency of mode 1. This points to a dominating role of mode 1 in the flutter mechanism. After passing the dip, the flutter frequencies increase again. Correlation with the trailing edge pressure curves shows that at the bottom of the dip the flow is still mainly attached, but that the right hand sides of the dips are influenced already by flow separation. The flutter characteristics for the condition $\alpha_0 = 2.05$ deg are very remarkable. Between the first and second dips, the flutter frequency increases rapidly to a value

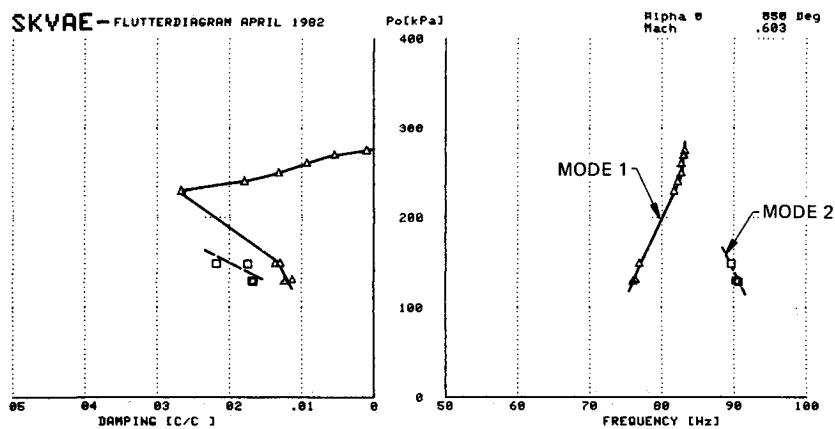
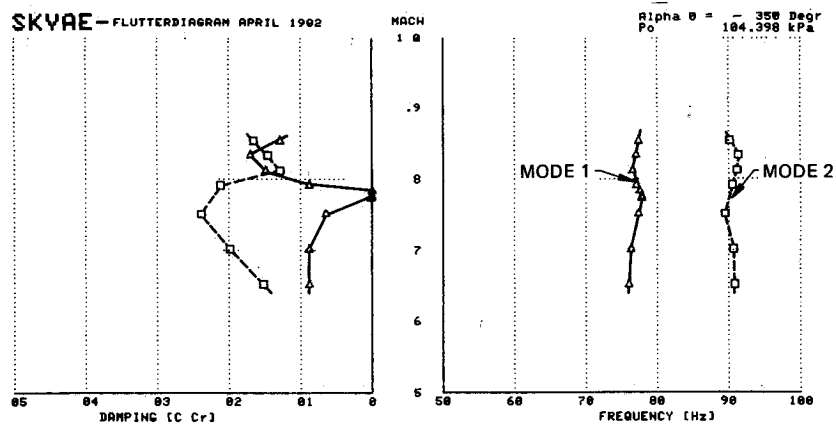
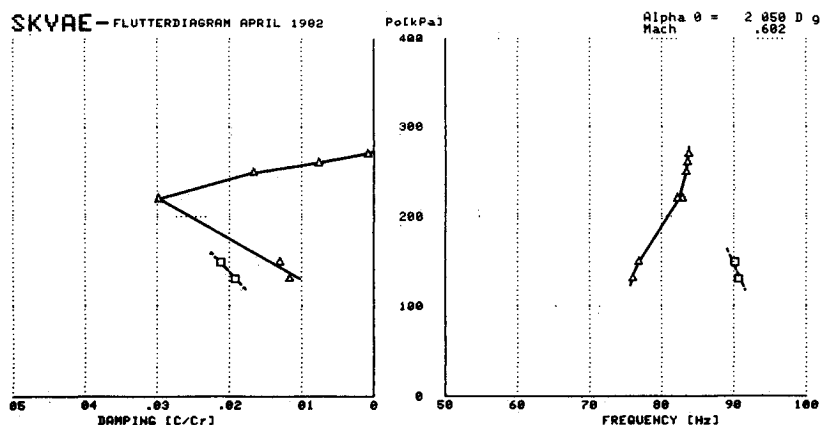
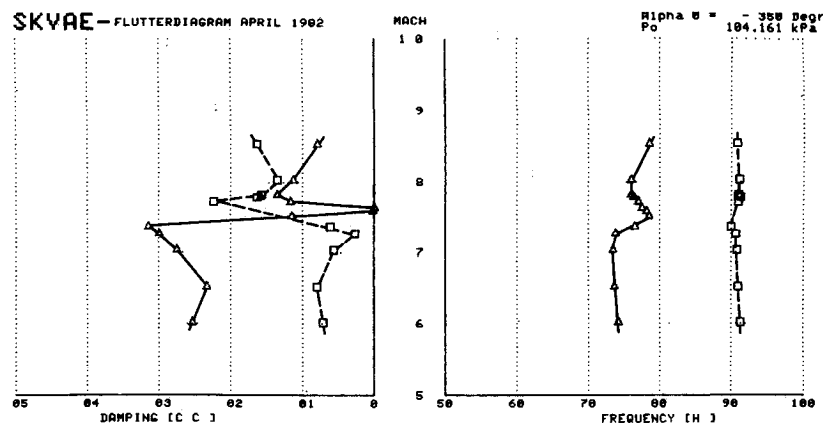


Fig 8 On line plotted flutter diagrams for $\alpha_0 = 0.85$ and 2.05 deg at subsonic flow (fixed transition)



FIXED TRANSITION

Fig 9 On line plotted flutter diagrams for $\alpha_0 = -0.35$ deg



NATURAL TRANSITION

Fig 10 On line plotted flutter diagrams for $\alpha_0 = 2.05$ deg (fixed transition)

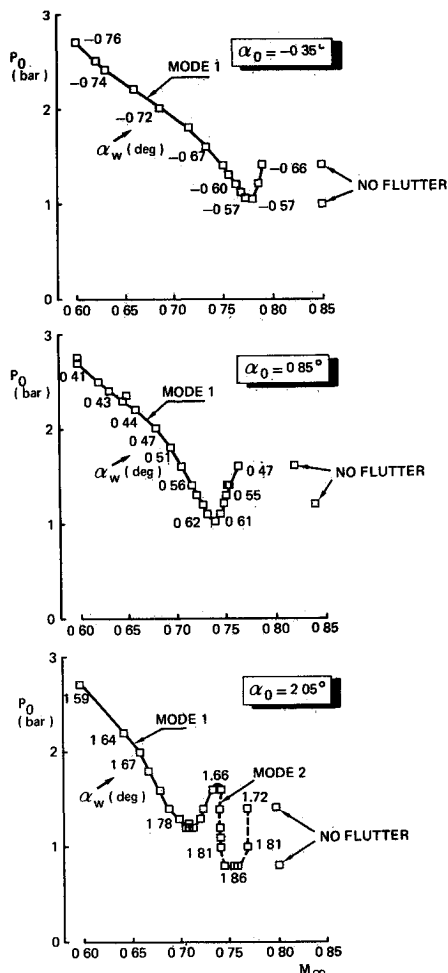
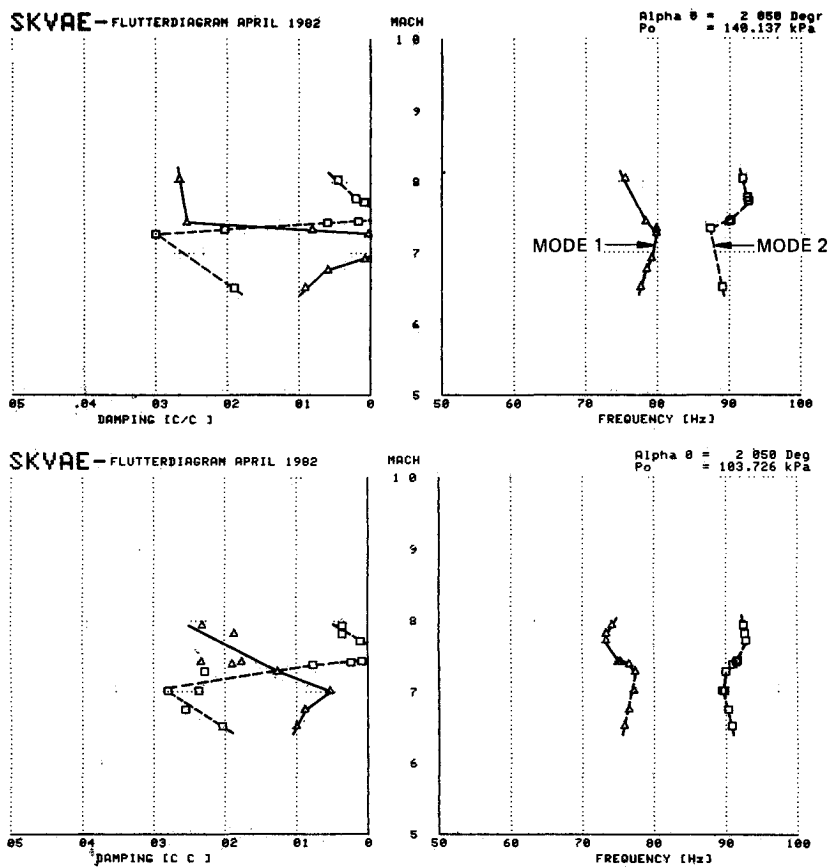


Fig 11 Measured flutter boundaries at $\alpha_0 = -0.35, 0.85$, and 2.05 deg (fixed transition)

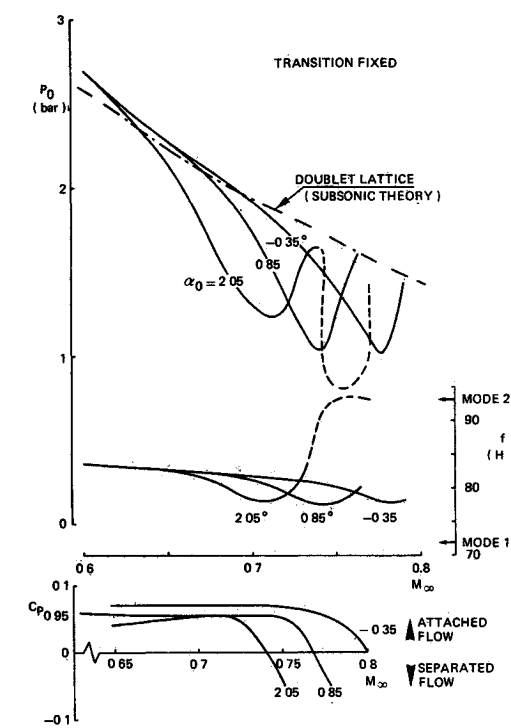


Fig 12 Survey of results from the wind tunnel flutter test

equal to the natural frequency of mode 2. This indicates that the flutter mechanism in the second dip is dominated almost completely by mode 2. Correlation with the trailing edge pressure curve shows that the instability takes place in separated flow.

Finally, the comparison with calculated flutter boundaries using the subsonic doublet lattice unsteady airloads method illustrates that, at $M_\infty = 0.6$, flutter onset is predicted with a somewhat conservative margin which is in agreement with experience of NLR and other flutter investigations.⁵ At transonic Mach numbers the flutter boundaries diverge strongly from the doublet lattice calculations.

Mean Pressure Distributions

The pressure distributions were compared with pressures from earlier steady pressure model tests. In this way the adjustment of the wing angles of attack (α_0) in the wind tunnel could be verified. Further separation onset was detected from the trailing edge pressures being an indication of whether the measured transonic dip was associated with attached or separated flow (see Fig. 12). The availability of this information immediately after each test run proved to be very helpful in understanding the flutter mechanism.

VII Conclusions

A wind tunnel flutter test was performed with a semispan model of a supercritical wing. The experiment was a continuation of a flutter test performed earlier with nearly the same model. Three wing angles of attack were investigated. The conclusions are as follows:

1) The flutter test was carried out very successfully. Measuring the model response and a mean pressure distribution simultaneously was of paramount importance to correlate flutter characteristics with the mean flowfield. Using on-line data reduction and presentation of flutter characteristics provided an adequate understanding of the test results and the possibility to adjust the measuring program, where necessary.

2) Using a flutter damper, the flutter boundaries could be measured very fast and accurately in a straightforward manner.

3) At $M_\infty \approx 0.6$, the measured flutter onset corresponding to the three wing angles of attack coincided so that the flow could be considered subsonic.

4) Above $M_\infty \approx 0.6$, the measured flutter boundaries diverged from doublet-lattice calculations due to high-subsonic and transonic effects.

5) Complete transonic dips were measured for each wing angle of attack. In the dip the flutter mechanism was governed mainly by a bending type mode of the model. The flow was attached. At the highest wing angle of attack a second dip was found in which the flutter mechanism was dictated completely by a torsion type mode while the flow was separated.

Acknowledgments

The work presented herein was carried out under contract with the Netherlands Agency for Aerospace Programs (NIVR). The authors acknowledge the Netherlands Agency for Aerospace Programs and the Netherlands Aircraft Factories Fokker B. V. for their permission to present the results.

References

- ¹Pronk, N., Walgemoed, H., and Zwaan, R. J., 'Transonic Flutter Clearance for a Supercritical Transport Aircraft in the Preliminary Design Stage', AGARD CP 354, Sept. 1983.
- ²Houwink, R., Kraan, A. N., and Zwaan, R. J., 'Wind Tunnel Study of the Flutter Characteristics of a Supercritical Wing', *Journal of Aircraft*, Vol. 19, May 1982, pp. 400-405.
- ³Zwaan, R. J., 'Verification of Calculation Methods for Unsteady Airloads in the Prediction of Transonic Flutter', AIAA Paper 84-0871, May 1984.
- ⁴User's Guide to the High Speed Wind Tunnel HST of the NLR, Revised edition, 1979, NLR, The Netherlands.
- ⁵Farmer, M. G., and Hanson, P. W., 'Comparison of Supercritical and Conventional Wing Flutter Characteristics', *Proceedings of the AIAA/ASME/SAE 17th Structures and Materials Conference*, King of Prussia, Pa., May 1976, pp. 608-614.